

Effect of protein fusion on the transition temperature of an environmentally responsive elastin-like polypeptide: a role for surface hydrophobicity?

K.Trabbic-Carlson¹, D.E.Meyer¹, L.Liu¹, R.Piervincenzi¹, N.Nath¹, T.LaBean¹ and A.Chilkoti^{2,3}

¹Department of Biomedical Engineering, Campus Box 90281 and

²Department of Computer Science, Campus Box 90129, Duke University, Durham, NC 27708, USA

³To whom correspondence should be addressed.

E-mail: chilkoti@duke.edu

The limited throughput, scalability and high cost of protein purification by chromatography provide motivation for the development of non-chromatographic protein purification technologies that are cheaper and easier to implement in a high-throughput format for proteomics applications and to scale up for industrial bioprocessing. We have shown that genetic fusion of a recombinant protein to an elastin-like polypeptide (ELP) imparts the environmentally sensitive solubility property of the ELP to the fusion protein, and thereby allows selective separation of the fusion protein from *Escherichia coli* lysate by aggregation above a critical temperature (T_t). Further development of ELP fusion proteins as widely applicable purification tools necessitates a quantitative understanding of how fused proteins perturb the ELP T_t such that purification conditions (T_t) may be predicted *a priori* for new recombinant proteins. We report here the effect that fusing six different proteins has on the T_t of an ELP. A negative correlation between T_t and the fraction hydrophobic surface area on the fused proteins was observed, which was determined from computer modeling of the available three-dimensional structure. The thermally triggered aggregation behavior of ELP-coated, functionalized gold colloids as well as ligand binding to the tendamistat-ELP fusion protein support the hypothesis that hydrophobic surfaces in molecular proximity to ELPs depress the ELP T_t by a mechanism analogous to hydrophobic residue substitution in the ELP repeat, Val-Pro-Gly-Xaa-Gly.

Keywords: aggregation/elastin/fusion protein/hydrophobicity/phase transition

Introduction

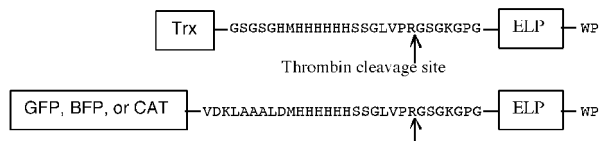
Elastin-like polypeptides (ELPs) (Urry, 1988, 1992, 1997) are artificial biopolymers containing repeats of the pentapeptide sequence Val-Pro-Gly-Xaa-Gly (VPGXG), where Xaa can be any naturally occurring amino acids except Pro (Pro substitution at the fourth position destroys the inverse phase transition) (Urry, 1992). This sequence is derived from the characteristic repeat motif, VPGVG, found in native, mammalian elastin. ELPs undergo an inverse phase transition: below their inverse transition temperature (T_t) ELPs are structurally disordered, highly solvated and therefore soluble in aqueous solutions, but as the temperature is raised the polymer gradually collapses and sheds bound water resulting in the formation of

intramolecular contacts between non-polar regions of the ELP (Li *et al.*, 2001a,b; Li and Daggett, 2003). At a critical temperature—the T_t —the ELP undergoes a phase transition, leading to aggregation of the polypeptide within a narrow temperature range (Urry *et al.*, 1985; Urry, 1992). It has been shown that the T_t values of ELPs are reduced by the incorporation of greater fractions of hydrophobic residues at the fourth, ‘guest’ residue (X), position of the repeat sequence, VPGXG, and that the magnitude of this effect is dependent not only on the mole fraction but also on the hydrophobicity of the guest residue. A linear correlation can be drawn between the ΔT_t and the mole fraction of the guest residue for any of the naturally occurring amino acids, thus providing a hydrophobicity scale for amino acids based solely on their effect on the T_t of ELPs (Urry *et al.*, 1991; Urry, 1992, 1997).

In previous studies, we showed that the environmentally sensitive solubility of ELPs is retained upon their fusion to other proteins (Meyer and Chilkoti, 1999; Meyer *et al.*, 2001b). Furthermore, because the phase transition of ELPs is reversible, ELPs can be used as reversible solubility tags to purify proteins from cell lysate. We have exploited the phase transition of ELP fusion proteins, to devise a simple, non-chromatographic means of purification, which we call inverse transition cycling, whereby a recombinant ELP fusion protein of interest can be separated from other contaminating *Escherichia coli* biomolecules in the soluble cell lysate by sequential and repeated steps of aggregation, centrifugation and resolubilization (Meyer and Chilkoti, 1999; Meyer *et al.*, 2001b). Because this purification method is carried out as a batch process, it can be easily scaled up for large-scale purification and also enables simultaneous purification of different proteins from multiple cultures.

We also observed in these studies that the T_t is modulated by the presence of the fused protein (Meyer and Chilkoti, 1999; Meyer *et al.*, 2001b). We observed that the T_t of a 36 kDa ELP without a fusion protein partner is ~51°C, but that its fusion to two different proteins results in greatly differing T_t of the ELP. Fusion of this ELP to the C-terminus of thioredoxin, a 12 kDa protein commonly used as a carrier to increase the solubility of recombinant proteins (Lavallie *et al.*, 1993), results in a 9°C elevation in T_t (60°C). In contrast, fusion of the same ELP to the N-terminus of tendamistat, an 8 kDa inhibitor of porcine pancreatic α -amylase (PPA) (Wiegand *et al.*, 1995), results in a 16°C depression in T_t (35°C) compared with free ELP. When these components are expressed as the ternary fusion protein thioredoxin-ELP-tendamistat (Trx-ELP-Tend), the T_t (34°C) is nearly identical to the T_t of the ELP-Tend binary fusion, and enzymatic cleavage of tendamistat from Trx-ELP-Tend results in a 26°C increase in T_t . Both these observations clearly suggest that the presence of tendamistat dominates the perturbation of T_t in the ternary fusion protein. We term this alteration of the T_t of an ELP upon fusion to a protein the ‘fusion ΔT_t effect’, [fusion $\Delta T_t = T_t$ (ELP fusion) – T_t (ELP)],

A. Binary ELP fusions - Trx, GFP, BFP, and CAT



B. Ternary ELP fusions -Trx-ELP-Tend

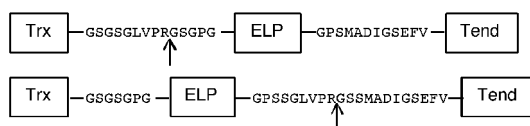


Fig. 1. Expressed sequences for ELP fusion proteins indicating the relative locations of the oligohistidine tag and thrombin cleavage sequences.

analogous to, but distinct from, the ΔT_i effect defined for the effect of ‘guest’ residue (X) substitution in the VPGXG repeat of ELPs (Urry *et al.*, 1991).

In this study, we have used diverse experimental and computational approaches to elucidate the biophysical principles governing this fusion ΔT_i effect. The hypothesis tested in this study, derived from previous observations (Meyer and Chilkoti, 1999), is that the fusion ΔT_i effect is controlled by the solvent-accessible hydrophobic area within molecular proximity of the ELP; exposed hydrophobic patches on the surface of proteins fused to ELPs alter the T_i of the ELP in a manner analogous to the ‘ ΔT_i effect’ whereby the T_i is depressed in proportion to the surface hydrophobicity of a fused protein. Understanding the biophysical basis of this fusion ΔT_i effect is important because it may enable the ΔT_i for a given ELP fusion protein to be quantitatively predicted *a priori*, from its structure or its physico-chemical properties. Discovering such quantitative structure–property correlations has practical implications, as well, for applications of ELP fusion proteins that exploit their phase transition behavior. For example, the ability to predict the T_i of an ELP fusion protein would be extremely useful in its purification by inverse transition cycling, because it will enable optimization of the purification protocol for a given protein without extensive trial and error.

Materials and methods

Synthesis of ternary ELP fusion genes

A synthetic gene with *SfiI*-generated, compatible sticky ends encoding for a 90 pentapeptide ELP was synthesized by recursive directional ligation in pUC-19 (Meyer and Chilkoti, 2002). The characteristic ELP repeat sequence of VPGXG contained 50% Val, 30% Gly and 20% Ala at the X position in this particular ELP and the DNA sequence for this gene has been published previously (Meyer and Chilkoti, 1999). A synthetic gene for tendamistat was assembled from three complementary sets of chemically synthesized oligonucleotides (5′ phosphorylated, PAGE purified; Integrated DNA Technologies), which were designed to provide *EcoRI* and *HindIII* complementary ends. The six oligonucleotides were annealed, in equimolar amounts, in a single reaction. The annealed product was separated by agarose gel electrophoresis and a ~230 bp band, corresponding to the length of the tendamistat gene, was excised and purified (Qiaex II Gel Extraction kit; Qiagen). The tendamistat gene was ligated into *EcoRI/HindIII* restricted and gel-purified pUC19 and transformed into XL1-Blue (Novagen) competent *E.coli*. Successful

transformants were identified by polymerase chain reaction (PCR) and subsequent DNA sequencing.

The tendamistat gene was inserted into a modified pET-32a expression vector (Novagen), which contains the thioredoxin gene. pET-32a was modified as follows: the S-tag peptide-coding region of the pET-32a vector was removed by replacement of the *MscI/NcoI* fragment with two alternate DNA cassettes, each encoding for a *SfiI* restriction site and the thrombin recognition site. The alternate ternary ELP constructs expressed from the two versions of the modified pET-32a vector allowed cleavage with thrombin either between thioredoxin and the ELP or between tendamistat and the ELP (Figure 1). The pUC19 plasmid containing the tendamistat gene was digested with *EcoRI* and *HindIII* and agarose gel purified to isolate the ~230 bp fragment. The modified pET-32a expression vector was digested with *EcoRI* and *HindIII*, treated with calf intestinal phosphatase (CIAP; Gibco, BRL), and ligated with the purified tendamistat *EcoRI/HindIII* insert. Ternary ELP fusion proteins were created by digestion with *SfiI* of the modified pET-32a plasmid containing the gene for the thioredoxin–tendamistat binary fusion, dephosphorylation of the digested vector with CIAP, followed by ligation of an insert containing the ELP gene with *SfiI*-compatible sticky ends. Standard molecular biology techniques were employed for all DNA manipulations (Ausubel *et al.*, 1995), and details regarding pET-32a DNA modifications and fusion protein construction have been published previously (Meyer and Chilkoti, 1999).

ELP fusions with green fluorescent protein (GFP), blue fluorescent protein (BFP) and chloramphenicol acetyltransferase (CAT) were synthesized by inserting the target gene 5′ to the ELP gene in a modified pET25b vector. The modified pET25b vector was produced by replacement of the *NotI* to *AvaI* segment of pET25b (Novagen) with an oligonucleotide cassette encoding for an oligohistidine tag, thrombin cleavage site, and a *SfiI* restriction site. The ELP gene was inserted into the *SfiI* restriction site as previously described (Meyer and Chilkoti, 1999), and details regarding the modified pET vector are available in the supplementary material (available at *PEDS* online).

BFP and GFP fusions with ELP were produced as follows. Plasmid DNA containing the genes for BFP (pQBIT7-BFP) and GFP (pQBIT7-GFP) were obtained from Qbiogene. Plasmids were digested with *XbaI* and *AlwNI*, and the first 723 bp of the BFP and GFP genes were isolated and purified from a low melting point agarose gel. A linker cassette with *AlwNI* and *SalI* compatible sticky ends encoding for the remaining 35 bp of the BFP and GFP genes was created from oligonucleotides (Integrated DNA Technologies). The modified pET25b vector containing the ELP gene was digested with *XbaI* and *SalI*, treated with CIAP, and purified from a low melting point agarose gel. Assembly of the fusion protein was accomplished by a ternary ligation of the 723 bp fragments of the BFP and GFP genes, the linker cassettes, and digested and purified pET25b vector. A pictorial representation of this cloning scheme and the sequence of the linker cassettes can be found in the supplementary material. Proper fusion protein assembly was confirmed by DNA sequencing.

The CAT gene was retrieved from its plasmid (provided by Invitrogen) by PCR and TA cloning (Invitrogen), in which *NdeI* and *SalI* restriction sites were also incorporated 5′ and 3′ to the gene, respectively. The gene was excised from the TA vector using *NdeI* and *SalI* and was purified from agarose gel.

The modified pET25b vector, previously described, was digested with *NdeI* and *SalI*, and the fusion protein was assembled by ligation of the CAT gene with the restricted pET25b vector containing the ELP gene. Correct fusion protein assembly was confirmed by DNA sequencing. The expressed peptide sequences for all the fusion protein constructs can be seen in Figure 1.

Expression and purification

The ternary ELP fusion proteins (Trx'ELP-Tend and Trx-ELP'Tend, where ' denotes the location of a thrombin cleavage site) were expressed from BL21trxB(DE3) *E. coli* (Novagen). The binary fusions of ELP to the C-terminus of BFP, GFP, CAT and Trx were expressed from BLR(DE3) *E. coli* (Novagen). All proteins were expressed in 1 l cultures of *E. coli* in CircleGrow™ media (Qbiogene, Carlsbad, CA, USA), supplemented with 100 µg/ml ampicillin. These 1 l cultures were inoculated with *E. coli* cells from 10 ml of a starter culture (250 ml flask containing 50 ml of medium supplemented with 100 µg/ml ampicillin) that was inoculated from frozen (-80°C) DMSO stocks and grown overnight. The 1 l cultures were grown either to an OD₆₀₀ of 0.8, induced with 1 mM isopropyl α -thiogalactopyranoside, and grown for an additional 3 h before being harvested or grown without induction for 24 h. Cultures were harvested by centrifugation at 4°C, resuspended in low ionic strength buffer (~1/25 culture volume), and lysed by ultrasonic disruption at 4°C. The lysate was centrifuged at ~20 000 g at 4°C for 15 min to remove insoluble matter.

Each ELP fusion protein was purified from soluble *E. coli* lysate using inverse transition cycling, a protein purification technique that we have previously developed (Meyer and Chilkoti, 1999). In a typical purification, the ionic strength of the soluble lysate was increased to cause aggregation of the ELP in the cell lysate at room temperature, and the aggregated ELP was separated from soluble *E. coli* proteins by centrifugation. The pellet containing the ELP coacervate was resuspended in cold PBS and centrifuged at 4°C to remove insoluble contaminants. This procedure of thermal cycling and centrifugation was repeated (usually three times) until the ELP was determined to be ~95% pure of *E. coli* contamination by visualization of Coomassie and/or copper-stained SDS-PAGE gels. Protein concentration was determined by UV-visible spectroscopy using extinction coefficients at 280 nm calculated from the primary amino acid sequence with the software program Protean (DNA Star).

Binary ELP fusion proteins were also obtained by enzymatic cleavage of two different Trx-ELP-Tend ternary fusion proteins, Trx-ELP'Tend and Trx'ELP-Tend, using thrombin (Novagen). Trx-ELP was obtained from the enzymatic cleavage of Trx-ELP'Tend, which contains a thrombin cleavage site located between the ELP and the tendamistat. ELP-Tend was obtained from the cleavage of a different ternary protein, Trx'ELP-Tend containing a thrombin cleavage located between thioredoxin and the ELP. Free ELP-A was obtained by enzymatic cleavage of ELP binary fusion protein (Figure 1), and free ELP-B was obtained by expression of the ELP with the N-terminal and C-terminal linker peptides used in ELP binary fusions (Figure 1). All proteins were cleaved overnight at room temperature from solutions at ~100 µM fusion protein using 10 U thrombin per µmole of fusion protein, and the cleavage products were purified by another round of inverse transition cycling.

Characterization of inverse temperature transition of ELP fusion proteins

The inverse transition temperatures of ELPs and ELP fusion proteins were measured on a Cary 300 UV-visible spectrophotometer equipped with a multicell thermoelectric temperature controller (Varian Instruments) by the change in optical density (OD) at 350 nm as the temperature was increased from 25 to 60°C at a heating rate of 1°C/min (Meyer and Chilkoti, 1999). The inverse transition temperature (T_i) was defined as the temperature at which the OD reached 50% of its maximum value.

The effect of PPA binding on the T_i of Trx-ELP-Tend, Trx-ELP and ELP-Tend was determined from turbidity measurements as a function of solution temperature. PPA (Roche) was obtained as a slurry in 3.2 M ammonium sulfate. Samples of 10 µM Trx-ELP-Tend, ELP-Tend and Trx-ELP were mixed in PBS with or without the presence of 10 µM PPA. Fusion protein concentrations were limited to 10 µM because of the approximate 12 µM solubility limit of PPA. Samples without PPA were supplemented with ammonium sulfate such that the buffer for all the samples was PBS with 320 mM ammonium sulfate.

Computer modeling

Protein Data Bank (PDB) files were selected from a representative group of 500 high-resolution structures (Lovell *et al.*, 2003) (<http://kinemage.biochem.duke.edu/databases/top500.php>). Nineteen PDB files were discarded from the data set because they were structures of either short peptides or subunits of multi-domain proteins. The PDB file names of the proteins are listed in the supplementary material. Total and hydrophobic surface area calculations were performed using the program PROBE (Word *et al.*, 1999) and a contact sphere with a 1.4 Å radius. The probe sphere was rolled over the outside of the protein and a contact dot was placed on the atomic surface where the water-sized probe contacted the protein without simultaneously intersecting the van der Waals shell of another atom. The contact surface was considered hydrophobic when the dot contacted any atom within the following residues having non-polar side chains: Ala, Cys, Ile, Leu, Phe, Trp, Tyr or Val, and the exposed hydrophobic surface area was calculated as a fraction of the hydrophobic dots relative to the total number of dots. PDB files 1gfl, 1bfp, 2trxA, 1noc, 1bvn and 1bvn were used to calculate the surface characteristics of GFP, BFP, Trx, CAT, tendamistat and PPA, respectively.

ELP-functionalized gold colloids

Hydrogen tetrachloroaurate(III)hydrate [HAuCl₄.xH₂O (99.99%)], 11-mercaptoundecanoic acid (MUA) and 1-undecanethiol (UDT) were purchased from Aldrich. The ELP used for these studies was a 71 kDa polypeptide with the repetitive pentapeptide sequence (Val-Pro-Gly-Xaa-Gly)₁₈₀ where Xaa was Val, Ala and Gly in the ratio of 5:2:3. This ELP has twice the chain length of the ELP used in the fusion proteins but has an identical composition.

All glassware used for preparation of gold colloids was thoroughly washed with aqua regia (3:1 HNO₃:HCl), rinsed extensively with distilled water and then dried in an oven at 100°C for 2 h. Colloidal gold was prepared by sodium citrate reduction of HAuCl₄ as reported earlier (Weisbecker *et al.*, 1996). Ten milliliters of a 1 mg/ml solution of HAuCl₄.xH₂O were added with vigorous stirring to 180 ml of boiling water in

a 500 ml round-bottomed flask fitted with a reflux condenser. After boiling resumed, 10 ml of a 10 mg/ml solution of sodium citrate in water were quickly added with continued stirring. The solution was boiled for another 20 min and then allowed to cool to room temperature, which resulted in the formation of a red suspension of colloidal gold. The suspension was filtered using a 0.22 μm filter (Corning, Corning, NY) and stored at 4°C until further use. The diameter of the gold colloids was determined to be ~13 nm by transmission electron microscopy, as previously described (Nath and Chilkoti, 2001).

The surface of the gold colloids was modified to be hydrophilic or hydrophobic by formation of a self-assembled monolayer (SAM) of a COOH-terminated thiol (MUA) or a CH₃-terminated thiol (UDT), respectively, on the surface of the gold colloid (Bain *et al.*, 1989; Weisbecker *et al.*, 1996). A suspension of the gold colloids was dialyzed overnight against 1 mM NaOH solution to remove excess citrate and chlorides from the solution. SAMs were prepared on the gold colloids by overnight incubation of a 1:1 (v/v) mixture of an aqueous suspension of colloidal gold and a 0.2 mM solution of MUA or UDT in absolute ethanol. Unreacted MUA and ethanol were removed from the COOH-functionalized gold colloids by centrifugation of the suspension at 14 000 *g* for 15 min, discarding the supernatant followed by resuspension of the colloids in 10 mM sodium phosphate buffer, pH 7.2 (PB). This step was repeated three times to ensure complete removal of the unreacted thiol and ethanol. Unreacted UDT and ethanol were removed from the CH₃-functionalized gold colloidal suspension by dialysis in distilled water; centrifugation of hydrophobic gold colloids was avoided because it causes their irreversible aggregation.

COOH-functionalized gold colloids were incubated with 1 mg/ml ELP in PB for 2 h, and then washed twice by centrifugation at 14 000 *g* with PB and finally resuspended in 0.6 ml of PB for further studies. CH₃-terminated gold colloids were incubated with 1 mg/ml ELP for 2 h. Unbound ELP was removed using centrifugal ultrafiltration (Centricon Millipore, Bedford, MA, USA) through a 100 kDa molecular weight cut-off filter.

Temperature-dependent behavior of ELP-functionalized gold colloids

The temperature-dependent aggregation of ELP-modified gold colloids was monitored by measuring the extinction spectrum as a function of temperature on a UV-visible spectrophotometer (Cary 300Bio; Varian Instruments), equipped with a thermoelectrically controlled multi-cell holder and temperature probe. The temperature was varied in 5°C increments over 10–40°C. A thermocouple was used to monitor the temperature of the solution in the cuvette. The extinction spectra were collected between 350 and 750 nm, and the normalized integrated extinction (NIE) between 600 and 750 nm was used as an indicator of aggregate formation. The NIE is defined as follows: $\text{NIE}(T) = (B_T - A)/A$, where *A* is the initial integrated extinction between 600 and 750 nm at 10°C before commencement of thermal cycling, and *B_T* is the integrated extinction between 600 and 750 nm at temperature *T* (Nath and Chilkoti, 2001).

Surface plasmon resonance (SPR)

For SPR measurements, glass coverslips were cleaned and a thin layer of Cr (20 Å) was thermally deposited under vacuum, followed by gold (500 Å). A carboxyl and methyl terminated SAM was prepared on the gold-coated glass coverslips by

overnight incubation in a 1 mM solution of MUA and UDT, respectively, in absolute ethanol.

SPR studies were performed on a BiacoreX instrument (Biacore AB, Uppsala, Sweden) on SAM-functionalized gold substrates on glass, which were mounted on empty BiacoreX cassettes using water-insoluble double-sided sticky tape (3M Inc.). The ELP was adsorbed onto a COOH-terminated and CH₃-terminated SAMs by perfusing a 1.0 mg/ml solution of the ELP (14.0 μM) at 1.0 $\mu\text{l}/\text{min}$, in 10 mM PB, pH 7.2 for 100 min at room temperature.

Results and discussion

Fusion of folded proteins alters the *T_i* of the ELP fusion partner

Trx–ELP–Tend fusion proteins containing the 90 pentapeptide ELP gene (Trx–ELP′Tend and Trx′ELP–Tend, where ′ indicates the location of thrombin cleavage site) were expressed and purified by inverse transition cycling. A portion of each ternary fusion protein was treated with thrombin to digest the Trx–ELP′Tend and Trx′ELP–Tend fusions into (Trx–ELP+Tend) and (Trx+ELP–Tend), respectively. Figure 2 shows the turbidity profiles for 25 μM solutions of Trx′ELP–Tend, Trx–ELP′Tend, their thrombin-cleaved products, and free ELP-A. Clearly, the location of the thrombin cleavage site does not alter the *T_i*, because both Trx′ELP–Tend and Trx–ELP′Tend, indicated by closed and open triangles, respectively, have overlapping turbidity profiles and a *T_i* of 34°C. Thrombin cleavage of both Trx–ELP–Tend variants reveals the individual contributions of thioredoxin and tendamistat to the altered *T_i* of the ternary fusion protein. Cleavage of the ternary fusion protein Trx–ELP′Tend to liberate tendamistat results in the binary Trx–ELP protein with a *T_i* of 60°C, which is 9°C higher than that of the free ELP. Liberation of thioredoxin from the ternary fusion protein Trx′ELP–Tend results in the binary fusion ELP–Tend having a *T_i* of 35°C, which is 16°C lower than that of the free ELP. The *T_i* of ELP–Tend (35°C) is very similar to the ternary fusion proteins (34°C), indicating that tendamistat has the dominant effect on the *T_i* of the ternary fusion proteins.

For all proteins investigated, thermal aggregation was reversible because the increase in turbidity with temperature was found to decrease upon cooling below *T_i*; ELP fusion proteins containing tendamistat exhibit reversibility up to 50°C and thioredoxin-containing ELP fusion proteins cleared after heating to 75°C, indicating that the increases in turbidity exhibited in Figure 2 are a result of the reversible aggregation of ELP and not the thermal denaturation of the fused protein. These results confirm the *T_i*s published previously for these ELP fusion proteins (Meyer and Chilkoti, 1999).

In a separate experiment (data not shown), we determined that free tendamistat in equimolar solution (i.e. after thrombin cleavage from the ternary fusion without subsequent purification steps) has no effect on the *T_i* of Trx–ELP, and likewise, free thioredoxin in solution has no effect on the *T_i* of ELP–Tend. Thus, the close proximity of fused proteins and not merely their presence in solution is responsible for the perturbation of the ELP *T_i*. These results led us to hypothesize that the molecular basis of these dramatic perturbations in *T_i* are connected with the interfacial properties of tendamistat and thioredoxin.

This same ELP was also fused to the C-terminus of Trx, GFP, BFP and CAT with the peptide linker sequence encoding

for an oligohistidine tag and a thrombin cleavage site shown in Figure 1A. Figure 3 shows the turbidity profiles of these fusion proteins as well as the turbidity profile of the free ELP-B at 25 μ M in PBS. Free ELP-B (with the binary fusion linker peptide shown in Figure 1A) exhibits a T_t of 48°C. Fusion of Trx, GFP and BFP resulted in the elevation of T_t to 54, 52 and 51°C, respectively, while fusion of CAT resulted in a depression to 36°C. Aggregation of Trx, BFP, GFP and CAT was completely reversible upon cooling after heating to 65°C. Fusion of CAT results in a broadening of the turbidity profile of the CAT-ELP fusion protein relative to the free ELP-B; the cause of this remains a mystery.

Short linker peptides also alter the T_t of ELP fusion proteins

Minor changes in amino acid sequence in the peptide linkers adjacent to but not explicitly part of the folded fused protein or the ELP can have significant effects on the ELP T_t . Figures 2 and 3 demonstrate that the addition of 23 amino acids including an oligohistidine sequence to the N-terminus of the ELP results in a 3°C depression in the ELP transition temperature. Trx-ELP fusion proteins expressed from two different constructs with two different peptide sequences at the N- and C-termini of the ELP also exhibit two different T_t s. Trx-ELP expressed as a binary fusion protein exhibited a T_t of 54°C (Figure 3) while Trx-ELP cleaved from the ternary fusion protein Trx-ELP-Tend had a T_t of 60°C (Figure 2) (Meyer and Chilkoti, 1999). Examination of the amino acid composition of these two

different expression products yields clues as to the source of this perturbation. Table I shows the leader and trailer sequences immediately flanking the ELP for two different sources of free ELP and Trx-ELP, their experimentally measured T_t s at 25 μ M in PBS, and their calculated hydrophobicity from the Urry hydrophobicity scale (Urry *et al.*, 1991; Urry, 1997).

The hydrophobicity of the leader and trailer sequence has been converted to a transition temperature scale using the correlation developed by Urry between guest residue (X) substitution in the VPGXG sequence and the T_t of the ELP (Urry *et al.*, 1991; Urry, 1997). This was achieved by taking a weighted average of the transition temperatures from the Urry hydrophobicity scale attributed to each of the residues in the leader and trailer sequence. We chose to use this temperature scale for hydrophobicity, so that the experimentally observed shifts in the T_t of the different variants of free ELP and Trx-ELP fusion protein, which only differed in their leader and trailer peptide sequence, could be directly correlated with the hydrophobicity of these peptide sequences. We note that the Urry hydrophobicity scale was originally developed to explain the effect of guest residue substitution in the ELP sequence VPGXG, and thus, the use of this scale as a predictive tool for the T_t of a non-ELP peptide (which would not exhibit an inverse phase transition itself) is somewhat meaningless. However, these predicted T_t s provide a general scale for the relative hydrophobicity of each peptidic leader and trailer combination, with lower calculated temperatures associated

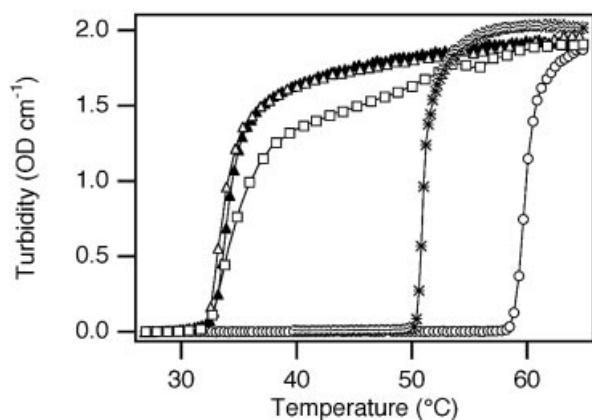


Fig. 2. Solution turbidity as a function of increasing temperature for 25 μ M solutions of ternary ELP fusions, Trx'ELP-Tend (open triangles) and Trx-ELP-Tend (closed triangles), their respective cleavage products after digestion with thrombin, ELP-Tend (squares) and Trx-ELP (circles) and free ELP-A (asterisks) in PBS showing T_t s of 34, 34, 35, 60 and 51°C, respectively.

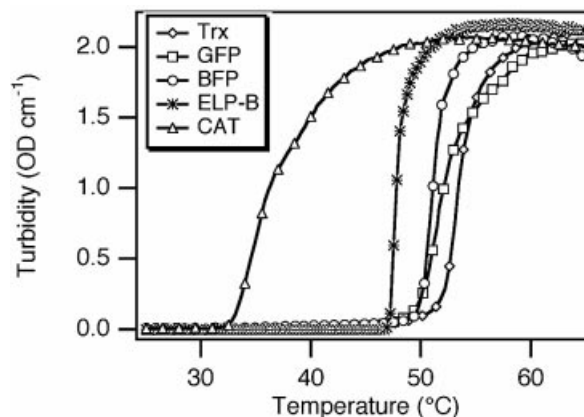


Fig. 3. Solution turbidity as a function of increasing temperature for 25 μ M solutions of binary ELP fusion protein solutions as well as the free ELP-B. The T_t of the free ELP-B is 48°C. The ELP T_t is depressed by fusion to CAT (36°C) and elevated by its fusion to Trx (54°C), GFP (52°C) and BFP (51°C).

Table I. Effect of leader and trailer sequence on the T_t of free ELPs and Trx-ELPs at 25 μ M in PBS

Protein	Source	Leader sequence	Trailer sequence	T_t (°C)	Calculated hydrophobicity (°C)
Free ELP-B	Expressed with the binary fusion leader and trailer peptides	VDKLAAALDMHHHHHHSSGLVPRGSGKGPG	WP	48	27
Free ELP-A	Cleaved from Trx'ELP	GSGKGPG	WP	51	32
Trx-ELP	Expressed as Trx'ELP	GSGSGMHHHHHHHSSGLVPRGSGKGPG	WP	54	25
Trx-ELP	Cleaved from Trx-ELP'Tend	GSGSGPG	GPSSGLVPR	60	40

Leader sequences are fused to the N-terminal of the ELP and span the gap between the C-terminus of Trx and the N-terminus of ELP in the Trx-ELP fusions. Trailer sequences are fused to the C-terminus of the ELP. A block diagram of fusion protein constructs can be seen in Figure 1. The hydrophobicities (°C) were calculated from the ELP hydrophobicity scale of Urry (Urry *et al.*, 1991; Urry, 1997) using a weighted average of the residues in the leader and trailer sequences.

with more hydrophobic sequences (Urry *et al.*, 1991; Urry, 1997).

The calculated hydrophobicities of the linker peptides qualitatively correlate with the experimentally measured transition temperatures of both the free ELP and Trx-ELP having different leader and trailer sequences. For both proteins (ELP and Trx-ELP) the lower measured T_t and calculated hydrophobicity are consistent with the assumption that the oligohistidine tag in the leader sequence is a major contributor to the hydrophobicity to that linker sequence. Although His is not considered to be particularly hydrophobic on many amino acid hydrophobicity scales (Fauchere and Pliska, 1983; Radzicka and Wolfenden, 1988; Roseman, 1988), Urry indicates that at pH 8.0, where His is largely uncharged, His is the fourth most hydrophobic amino acid (Urry, 1992, 1997) on the ELP hydrophobicity scale. Because the pK_a of His falls somewhere between 6.0 and 7.0 (Bundi and Wuthrich, 1979; Matthew *et al.*, 1985), we expect the majority of histidines to be uncharged and hydrophobic at our working pH of 7.4. We have, therefore, used the uncharged values for histidine hydrophobicity in our calculations from the Urry scale. With this assumption, we observe that the hydrophobicity of the leader and trailer peptide sequence is consistent with the differences in the measured T_t s of free ELPs and Trx-ELP fusion proteins containing different linker peptides.

Functionalized gold colloids as a probe of the effect of proximity of solid interfaces on the ELP T_t

We chose to use gold colloids as a mimic of the interfacial properties of proteins for the following reasons. First, they can be synthesized in size ranges that approximate that of proteins (~5 nm and larger). Secondly, the interfacial properties of gold colloids can be easily modified by the formation of SAMs of alkanethiols; surfaces can be created via formation of SAMs that are hydrophobic, hydrophilic or chemically reactive, and these surface properties of gold can be further tuned by the formation of mixed SAMs. Finally, as shown previously, the phase transition of ELPs adsorbed or covalently conjugated to gold colloids can be conveniently monitored colorimetrically by the SPR of gold colloids (Kreibig and Vollmer, 1995). This is because aggregation of ELP-modified gold colloids, owing to the hydrophilic-hydrophobic phase transition of the ELP, results in a dramatic change in color of the colloidal suspension from red to violet, and monitoring the wavelength shift of the extinction spectrum or the intensity at a fixed wavelength provides a simple read-out of the interfacial phase transition behavior of ELPs (Nath and Chilkoti, 2001). Hence, these properties of gold colloids suggested their use as a simple model system, within the context of this study, to examine the effect of interfacial hydrophobicity (at a dimensional scale roughly commensurate with that of proteins) on the phase transition behavior of ELPs. Because the size of the gold colloids is roughly twice that of most of these fusion proteins, we used an ELP to functionalize the colloids that has twice the MW (71 kDa) of the ELP in the fusion proteins. This ELP has the same chemical composition and exhibits a similarly sharp inverse transition as the ELP in the fusion proteins. The only relevant difference in its properties from the shorter ELP is that it has a T_t that is 10°C lower (at 25 μ M in PBS), which is a direct consequence of its larger MW (Meyer and Chilkoti, 2002). Because these ELPs are so similar in their solution transition behavior and have identical compositions, we expect similar surface transition behavior as well.

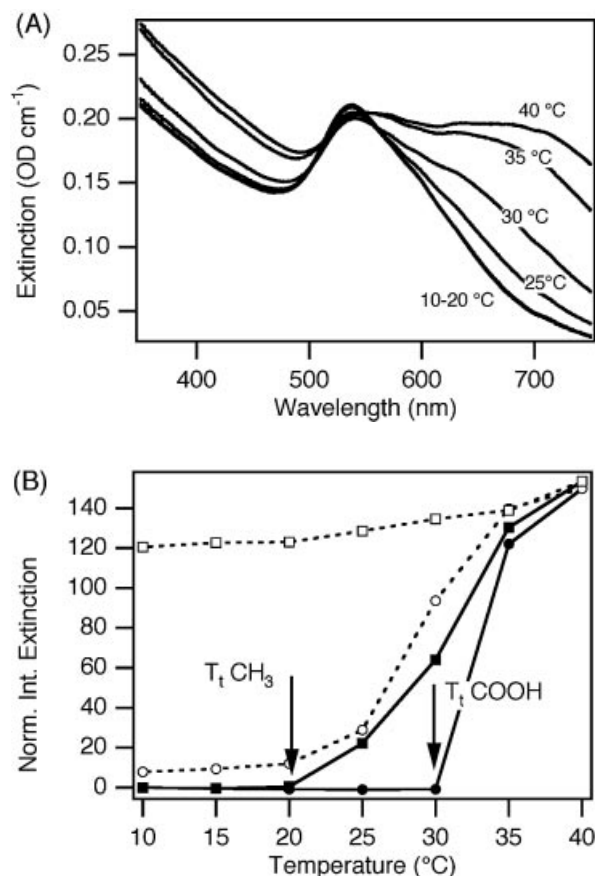


Fig. 4. (A) Extinction spectrum of gold colloids functionalized with a CH_3 -terminated SAM and adsorbed ELP as a function of increasing temperature. (B) Change in the NIE of gold colloids functionalized with COOH-terminated SAM (circles) or CH_3 -terminated SAM (squares) and adsorbed ELP as a function of solution temperature during heating (closed markers with solid lines) and cooling (open markers with dashed lines) showing the onset of the ELP phase transition at $\sim 20^\circ\text{C}$ for the hydrophobic surface and $\sim 30^\circ\text{C}$ for the hydrophilic surface.

We adsorbed the ELP onto gold colloids that were modified with either a COOH-terminated SAM or a CH_3 -terminated SAM. These SAMs were chosen to make the surface of the gold colloids hydrophilic (COOH-terminated SAM) or hydrophobic (CH_3 -terminated SAM). Figure 4A shows the extinction spectrum of an aqueous suspension of gold colloids, functionalized with a CH_3 -terminated SAM and adsorbed ELP, as a function of increasing solution temperature. Below a solution temperature of 20°C , the extinction spectrum does not vary with temperature. Above 20°C , however, the extinction spectra exhibit a shift in the extinction maximum towards higher wavelengths and an increase in the absolute intensity at wavelengths above 600 nm. The NIE, the area under the peak from 600 to 750 nm, is shown in Figure 4B for the adsorbed ELP on the COOH-terminated SAM on colloidal gold (circles) and CH_3 -terminated SAM (squares). The ELP adsorbed onto the COOH-terminated SAM exhibits a sharp and reversible phase transition similar to its behavior in solution, with a T_t of $\sim 30^\circ\text{C}$. In contrast, ELP adsorbed onto the CH_3 -terminated SAM exhibits significantly different thermal behavior. First, its T_t is depressed by $\sim 10^\circ\text{C}$ compared with the COOH-terminated SAM, and secondly, the phase transition is irreversible. The T_t is defined by the onset of the transition from the baseline of the NIE because, unlike turbidity measurements, the maximum

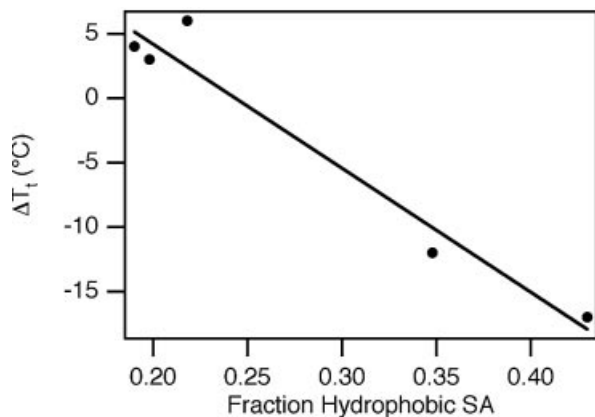


Fig. 5. The effect of fraction hydrophobic surface area on the fusion ΔT_t effect for the following proteins fused to an ELP: GFP, BFP, Trx, CAT and tendamistat.

NIE measured for each of the surfaces does not necessarily represent a saturation in the spectral changes of the colloids as a function of temperature. The decrease in the T_t , when the surface presented to the ELP by the gold colloids is changed from hydrophilic to hydrophobic, is consistent with the hypothesis that an increase in interfacial hydrophobicity lowers the T_t of an ELP.

Solution studies of free ELPs have shown that their T_t is inversely proportional to the logarithm of their concentration in solution (Meyer *et al.*, 2001a). Thus, we investigated whether the T_t of ELP-modified gold colloids might be a stronger function of the surface concentration of the ELP adsorbed on the different colloids rather than the interfacial properties of the gold colloids. While the surface density of adsorbed ELP on COOH- and CH₃-modified gold colloids could not be directly measured, SPR spectroscopy was used to quantify the surface concentration of ELP adsorbed on a thin film of gold that was identically modified with COOH- and CH₃-terminated thiols. Results from SPR performed using the same buffer and ELP concentration (Nath and Chilkoti, 2001) for ELP adsorption indicate an ELP surface concentration of ~ 5.0 ng/mm² of ELP on the COOH-terminated SAM and 2.5 ng/mm² on the CH₃-terminated SAM (Nath and Chilkoti, 2001). Thus, if the concentration of adsorbed ELP were alone responsible for the difference in ELP T_t , the ELP adsorbed on the COOH-terminated SAM should exhibit a lower T_t . In contrast, the adsorbed ELP exhibits a lower T_t on the CH₃-terminated SAM. These results strongly indicate that colloid surface characteristics and not adsorbed ELP concentration play the dominant role in determining the interfacial T_t of adsorbed ELPs.

The fusion ΔT_t effect

Analogous to the means by which the proximity of a hydrophobic interface such as a hydrophobic gold colloid can perturb the T_t of an ELP, we hypothesize that covalently attached proteins and peptides alter the T_t of an ELP by a similar mechanism: fused proteins provide a surface in close proximity to the ELP, and the presence of hydrophobic residues on that surface depresses the ELP T_t . If this hypothesis is valid, then fused proteins of differing hydrophobic character should exhibit differing effects on the ELP T_t , and deliberate

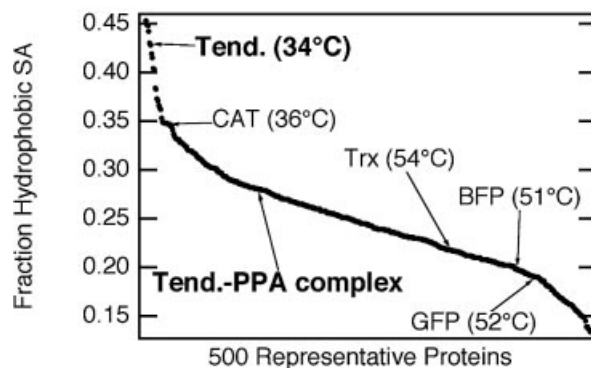


Fig. 6. Hydrophobic fraction of solvent-accessible surface ($SAS_{hydrophobic}/SAS_{total}$) for 500 protein structures (of greater than 40 amino acid residues) selected from the PDB showing the high fraction hydrophobic surface area for ELP fusion proteins highlighting the relative positions and transition temperatures (at 25 μ M in PBS) of tendamistat and the tendamistat-PPA complex.

alterations in the surface hydrophobicity of fused proteins should perturb this effect on the T_t of the fused ELP.

We quantified the total and fraction hydrophobic solvent-accessible surface area ($SAS_{hydrophobic}$) of ELP fusion proteins using PROBE (Word *et al.*, 1999). Using this program, the surface of a protein is interrogated by a rolling sphere with a 1.4 Å radius, corresponding to the radius of a water molecule, and the surface character is mapped according to its hydrophobicity. The surface is considered to be hydrophobic when the probe contacts residues having the following non-polar side chains: Ala, Cys, Ile, Leu, Phe, Trp, Tyr or Val. The fusion ΔT_t effect for each protein was determined by taking the T_t of the fusion protein and subtracting the T_t of the most appropriate free ELP control. All T_t s were measured at 25 μ M in PBS. For GFP, BFP, Trx and CAT, which were all expressed as binary fusions, an ELP T_t of 48°C corresponding to the ELP T_t expressed with the N-terminal linker peptide was used. For ELP-Tend, which was produced from the enzymatic cleavage of Trx'ELP-Tend, a T_t of 51°C, corresponding to an ELP lacking the His-tag linker peptide, was subtracted to compute ΔT_t for these ELP fusion proteins.

Figure 5 shows the fusion ΔT_t of the binary ELP fusion proteins GFP, BFP, Trx, CAT and tendamistat as a function of $SAS_{hydrophobic}$ and these data exhibit a linear correlation between fusion ΔT_t and $SAS_{hydrophobic}$ with a slope of $-96^\circ\text{C}(\text{fraction } SAS_{hydrophobic})^{-1}$ and a χ^2 error of 20.4. Attempts to correlate the fusion ΔT_t effect with the total $SAS_{hydrophobic}$ rather than the fraction $SAS_{hydrophobic}$ resulted in substantially higher correlation errors ($\chi^2 = 350$) suggesting that T_t is far more closely correlated with the composite surface characteristics of the fused protein rather than the total hydrophobic surface area.

Furthermore, comparison of the surface and bulk hydrophobicity provides compelling evidence that surface properties likely play a dominant role in modulating the T_t . Tendamistat and thioredoxin have widely differing surface hydrophobicities, with thioredoxin having a relatively hydrophilic surface at 22% $SAS_{hydrophobic}$ and tendamistat having among the most hydrophobic surfaces of all the proteins investigated at 43% $SAS_{hydrophobic}$. However, examination of the total amino acid content of both proteins indicates that thioredoxin and tendamistat are very similar in the hydrophobicity of their

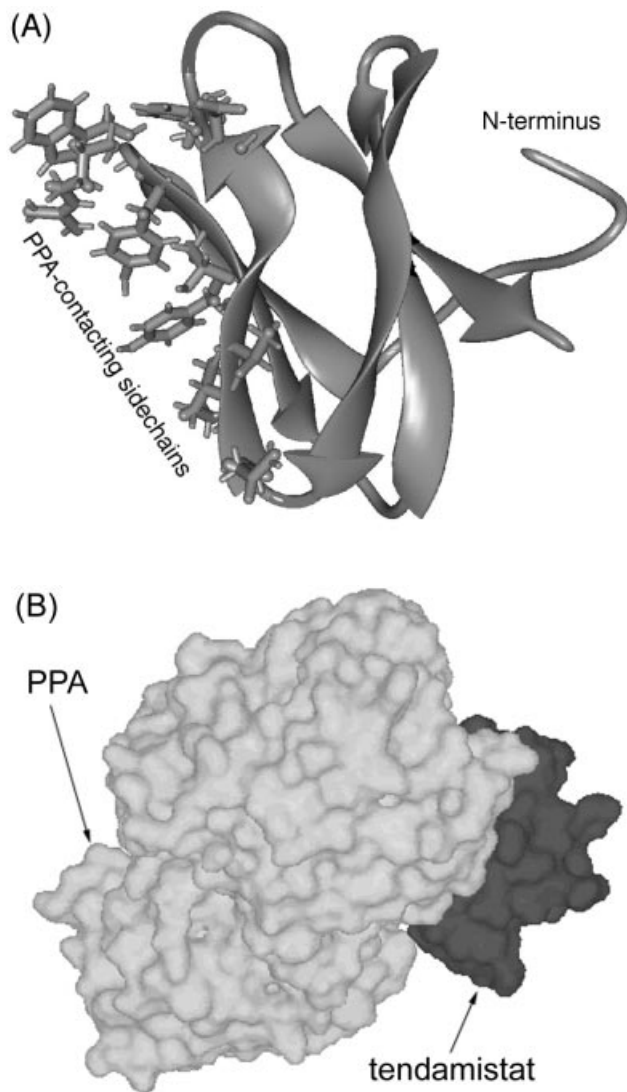


Fig. 7. (A) Ribbon diagram of tendamistat rendered from its crystal structure (Pflugrath *et al.*, 1986) showing relative positions of the PPA binding region and the N-terminus where the ELP is fused. (B) Solvent-accessible surface of PPA-tendamistat complex (Wiegand *et al.*, 1995) displayed in an orientation where tendamistat is oriented similarly to the ribbon structure in (A).

total composition, as both proteins have nearly equal total hydrophobic amino acid content at 44 and 45% by weight for tendamistat and thioredoxin, respectively. Thus, the surface properties of these two proteins, consequences of their folded, three-dimensional structures, are likely responsible for their widely differing effects on the T_t of their ELP fusions.

To gain a better understanding of the relative degrees of hydrophobicity for each of these proteins within a broader context, we calculated the fraction hydrophobic surface area for a group of nearly 500 proteins with high quality crystal structures. Figure 6 shows the fraction hydrophobic surface area for this representative group and highlights the values for the proteins of interest. Tendamistat and CAT are grouped at the hydrophobic end of this representative group, with tendamistat being among the most hydrophobic of all the proteins examined, while GFP, BFP and Trx are grouped at the opposite, hydrophilic end. The PPA-tendamistat complex has

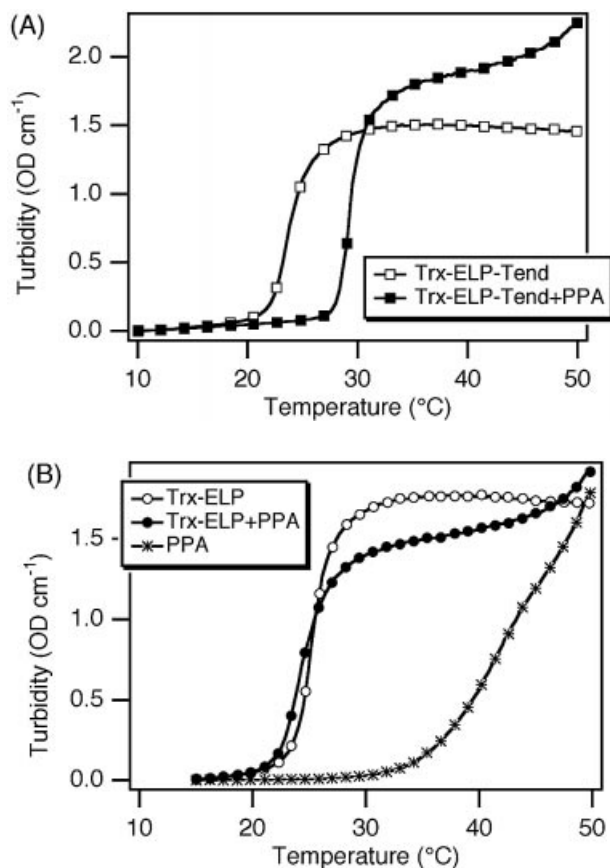


Fig. 8. Heating turbidity profiles of 10 μ M ELP fusion proteins with and without 10 μ M PPA in PBS + 320 mM ammonium sulfate showing (A) the elevation in the transition temperature of Trx-ELP-Tend in the presence of PPA and (B) the very slight depression in the T_t of Trx-ELP in the presence of PPA. The addition of PPA causes a 5.5°C increase in the T_t of Trx-ELP-Tend while the effect of PPA on the T_t of Trx-ELP is negligible with only a 0.7°C decrease in the presence of PPA. The increase in PPA turbidity above 30°C is caused by its irreversible thermal denaturation, and thus the increases in the turbidity of fusion protein solutions containing PPA above 30°C can be attributed to PPA denaturation.

an intermediate surface hydrophobicity in the database of approximately 500 proteins. From these calculations, we hypothesize that ELP fusion proteins containing tendamistat would exhibit a higher T_t upon binding to PPA.

Burial of a solvent-accessible hydrophobic patch in tendamistat upon binding of PPA reduces the fusion ΔT_t effect

To experimentally test this hypothesis, we deliberately altered the surface properties of the Tend-ELP fusion proteins by binding tendamistat to PPA and measuring the effect of complexation on the T_t of the fusion protein. Tendamistat, a strong competitive inhibitor of PPA, is a small protein (8 kDa) with a very large fraction of exposed hydrophobic surface (43%) (Wiegand *et al.*, 1995). Tendamistat contacts PPA over a large surface area ($\sim 1330 \text{ \AA}^2$), and its high affinity for PPA is derived largely from the exclusion of water from much of the hydrophobic interface that contacts PPA (Wiegand *et al.*, 1995). Figure 7A shows the tertiary structure of tendamistat including its large solvent-exposed, hydrophobic PPA binding site. PPA, its binding partner, is a considerably larger protein (55 kDa) that hydrolyzes the α -1,4-glucan link in starch to form maltose (Wiegand *et al.*, 1995). Figure 7B shows the exposed solvent-accessible surface of the PPA-tendamistat

complex and the relative sizes of the two proteins. Upon binding, solvent is excluded not only from the partially hydrophobic binding pocket of PPA but also from the highly hydrophobic binding ridge in tendamistat, and the resulting tendamistat–PPA complex has a hydrophobic surface area of 28%.

Figure 8A shows the heating turbidity profiles for Trx–ELP–Tend, with and without PPA. The addition of PPA causes a 5.5°C increase in the T_t of Trx–ELP–Tend (29.3°C) consistent with the increase in surface hydrophilicity calculated from structural modeling data. A similar 7°C increase in the T_t of ELP–Tend was observed upon binding to PPA (results not shown). Figure 8B shows the heating turbidity profiles of Trx–ELP with and without PPA as well as that of PPA alone. PPA has no significant effect on the T_t of Trx–ELP. Its presence in solution causes, at most, a 0.7°C depression in the T_t of Trx–ELP. The increase in PPA turbidity above 30°C results from its irreversible thermal denaturation, which is responsible for the secondary increase in turbidity observed above 40°C for samples containing PPA. These results clearly show that the effect of PPA on the T_t of Tend–ELP is caused by binding of the enzyme to its inhibitor and is not a non-specific effect as a result of the addition of a cosolute (i.e. PPA) to the solution. This T_t shift likely reflects a near 100% complexation of the Tend–ELP with PPA because of tendamistat's very high inhibition constant of 9×10^{-12} M (Wiegand *et al.*, 1995). This assumption is corroborated by the shape of the turbidity file. Previous studies have shown that mixtures of ELPs with different T_t s exhibit independent transitions which can be detected in the shape of the turbidity profile (Meyer and Chilkoti, 2002). If uncomplexed Tend–ELP fusion proteins were also present in solution, we would anticipate that the turbidity profile would exhibit independent transitions corresponding to the T_t of the free and bound states of tendamistat. The shape of these turbidity profiles suggests that the Trx–ELP–Tend (and the ELP–Tend, not shown) are present in a single, PPA-bound state when PPA is present in solution.

This experiment demonstrates several key points in our understanding of the effect of fused proteins on ELP T_t . First, this experiment clearly demonstrates that the fraction $SAS_{\text{hydrophobic}}$ is correlated with the fusion ΔT_t effect and not the total $SAS_{\text{hydrophobic}}$. Because PPA has nearly seven times the mass of tendamistat, PPA binding results in a 3-fold increase in the total $SAS_{\text{hydrophobic}}$ and a 2-fold decrease in the fraction $SAS_{\text{hydrophobic}}$. This elevation in T_t with a decrease in the fraction $SAS_{\text{hydrophobic}}$ is consistent with changes in T_t for the simple binary fusion proteins shown in Figure 5.

These results also highlight the potential importance of electrostatics on the fusion protein T_t . Previous studies have clearly shown that the T_t s of ELPs and ELP fusion proteins are depressed by the addition of salts (Urry, 1993; Meyer *et al.*, 2001b). This is also evident by comparing the T_t s of Trx–ELP–Tend and Trx'ELP measured from the turbidity profiles in Figures 2, 3 and 8. The relatively low T_t s in Figure 8 result from the addition of 320 mM ammonium sulfate from the PPA storage solution to maintain the activity of the PPA as recommended by the supplier (Roche). Ammonium sulfate solutions have ionic strengths three times greater than solutions having equivalent molar concentrations of NaCl. The amplified depression in fusion protein T_t with relatively small amounts of ammonium sulfate is consistent with the shielding of surface charges on fused proteins and the effect of multivalent anions on the inverse phase transition of the ELP itself. While

ammonium sulfate causes a depression in T_t for both Trx–ELP–Tend and Trx'ELP, the magnitude of the depression is significantly higher for Trx'ELP. Trx–ELP–Tend and ELP–Tend (data not shown) exhibit a 10°C depression in T_t upon the addition of 320 mM ammonium sulfate, but Trx'ELP exhibits a 29°C depression. This observation suggests that electrostatics likely play a larger role in the aggregation behavior of Trx–ELP fusion proteins compared with Tend–ELP fusions.

Because hydrophobic surfaces only account for negative changes in T_t , the fraction $SAS_{\text{hydrophobic}}$ alone cannot explain the increase in the T_t of an ELP upon fusion to a protein. BFP, GFP and Trx cause an elevation in the ELP T_t upon their fusion. Previous studies have clearly shown that incorporation of polar, hydrophilic and charged amino acids at the fourth 'guest residue' position in the VPGXG repeat of ELPs elevate the T_t of ELP. Charged moieties produce the most dramatic increases in ELP T_t , with the charged forms of Lys, Asp and Glu causing the greatest increase in ELP T_t when substituted at the guest residue position (Urry *et al.*, 1991; Urry, 1997). In fact, the phosphorylation of a single Ser residue in an ELP of 81 amino acids increases the T_t of an ELP by 12°C (Pattanaik *et al.*, 1991; Urry, 1992). By analogy, we suggest the presence of these solvent-accessible polar and charged groups on the surface of the fusion partner competes with the negative effect of hydrophobic surfaces. Thus, the T_t of a particular ELP fusion protein likely arises from combination of the negative effects of hydrophobic surface area and positive effects of charged and/or polar surface area with charged residues being of particular importance. Although tendamistat and Trx have very similar calculated (DNA star) pI s of 4.4 and 4.5, respectively, the inverse transition behavior of Trx–ELP, which has a substantially smaller fraction $SAS_{\text{hydrophobic}}$, is more heavily dominated by its charged/polar groups, as evident by its high salt sensitivity and its positive shift in T_t relative to free ELP at 25 μ M in PBS.

Proposed mechanism of the 'fusion ΔT_t ' effect

Urry and colleagues have shown that the local environment of the ELP chain, and the degree of hydrophobic hydration, can be directly modulated by substitution of natural or unnatural amino acids for the Val that is normally present in native elastin; the T_t s of ELPs are reduced by the incorporation of hydrophobic residues and the T_t is increased by polar and charged residues at the fourth, 'guest' residue (X), position of the repeat sequence, VPGXG. The magnitude of this effect (the ' ΔT_t effect') is dependent not only on the mole fraction but also on the hydrophobicity of the guest residue (Urry *et al.*, 1991; Urry, 1992, 1997). The 'fusion ΔT_t effect' reported here is analogous to, but distinct from, the ' ΔT_t effect' (Urry *et al.*, 1991; Urry, 1992, 1997) in which the hydrophobicity of the guest residues within the ELP chain modulates the T_t ; in contrast, the 'fusion ΔT_t effect' is one in which the ELP T_t is modulated by hydrophobic moieties not within the ELP chain but those closely associated with it.

As suggested by the molecular dynamics simulations of Daggett and colleagues (Li *et al.*, 2001a,b; Li and Daggett, 2003) and the microwave dielectric relaxation measurements of Urry *et al.* (1997), the release of water molecules of hydrophobic hydration from the ELP with increasing temperature is the dominant molecular contributor to providing the thermodynamic driving force for the ELP phase transition. We believe that the interfacial waters of hydration solvating hydrophobic patches within molecular proximity to an ELP

as well as the waters of hydrophobic hydration surrounding the ELP itself constitute the total number of waters that act in unison in response to an increase in the solution temperature. These surfaces include, but are not limited to, hydrophobic patches on the surfaces of fused folded proteins, short hydrophobic peptides fused to ELPs, or other hydrophobic surfaces within molecular proximity (i.e. hydrophobic gold colloids). Hence, with increasing temperature, the water molecules of hydrophobic hydration solvating the ELP chain as well as any closely associated with a hydrophobic surface are released to bulk. That the T_t of the ELP fusion protein is lowered relative to the ELP is simply a consequence of the release of the additional water molecules of hydrophobic hydration contributed by the fusion partner, which provides an additional gain in entropy per ELP chain upon their release to bulk.

Likewise, charged residues compete for waters of hydrophobic hydration (Urry, 1992). Fusion proteins having a low fraction $SAS_{\text{hydrophobic}}$ and a greater fraction of charged residues exhibit a positive shift in ELP T_t consistent with this competition for waters of hydrophobic hydration. The smaller gain in entropy for this class of fusion proteins upon desolvation, relative to the ELP, is then reflected in the greater T_t of the fusion protein. An implicit set of assumptions that underlie this analysis are: (i) the ELP phase transition in a fusion protein is a first-order phase transition; (ii) the ΔH of the phase transition for the ELP fusion protein is similar in magnitude to that of the ELP and is weakly endothermic (Luan et al., 1990, 1992), so that the change in enthalpy is not the dominant factor in modulating the T_t ; (iii) the conformational entropy of the ELP upon fusion is not significantly different from that of the ELP.

Conclusions

The results presented in this paper clearly show that surfaces held in close molecular proximity to ELPs cause dramatic changes in the T_t of the ELP and that the degree to which the ELP T_t is altered is proportional to the net hydrophobic character of the surface consistent with this entropically driven mechanism. Several examples illustrate this effect. First, fusion of ELP to CAT and tendamistat, proteins with relatively hydrophobic surfaces, significantly depresses the T_t , while fusion to GFP, BFP and Trx, which have relatively hydrophilic surfaces, elevates the T_t of ELP. This effect is only observed when the proteins are covalently attached to the ELP, and is not observed when equimolar amounts of the same species are present in bulk solution, highlighting the importance of molecular proximity. Secondly, small peptide sequences immediately adjacent to the ELP, which also provide proximal surfaces, also perturb the T_t of the ELP in a manner consistent with their mean residue hydrophobicity. Thirdly, ELP adsorbed onto gold colloids modified with a hydrophobic CH_3 -terminated SAM exhibited a T_t 10°C lower than the same ELP adsorbed onto a hydrophilic COOH-terminated SAM. Finally, this qualitative mechanism also explains the increase in the T_t of Tend-ELP upon binding of PPA, relative to the unbound fusion protein. Upon complexation with PPA, water molecules of hydrophobic hydration present at the hydrophobic binding patch of tendamistat are lost from the protein. Hence, they are not available for release during the thermally triggered desolvation of the ELP, so that the net gain in entropy per ELP is smaller, which requires a larger,

compensating T_t to drive the phase transition in the PPA complex of Tend-ELP.

The effect that fused proteins have on the T_t of ELPs is likely a complex one with charged and polar surface residues elevating and hydrophobic residues depressing T_t . Studies currently under way will further explore the effect of electrostatics on fusion protein T_t . These studies will help identify the optimal ELP tag and environmental conditions for protein purification based on the physico-chemical properties of the fusion partner. Finally, we note that aside from the insights it provides on the molecular origins of the fusion ΔT_t effect, the altered T_t of Tend-ELP upon binding of PPA is also interesting because it is the first demonstration, to our knowledge, of molecular recognition-mediated modulation of an ELP phase transition. We believe that modulation of an ELP fusion protein by ligand binding is likely to be useful for diverse applications in biotechnology including protein purification, ligand capture and biocatalysis.

Acknowledgements

The gene for CAT was graciously donated by Dr Jon Chesnut at Invitrogen. We thank the National Institutes of Health (GM-061232) for their financial support of this research.

References

- Ausubel, F.M. et al. (1995) *Current Protocols in Molecular Biology*. John Wiley and Sons, New York.
- Bain, C.D. et al. (1989) *J. Am. Chem. Soc.*, **111**, 321–335.
- Bundi, A. and Wuthrich, K. (1979) *Biopolymers*, **18**, 285–297.
- Fauchere, J.L. and Pliska, V. (1983) *Eur. J. Med. Chem.*, **18**, 369–375.
- Kreibig, U. and Vollmer, M. (1995) *Optical Properties of Metal Clusters*. Springer-Verlag, New York.
- Lavallie, E.R. et al. (1993) *Biotechnology*, **11**, 187–193.
- Li, B. and Daggett, V. (2003) *Biopolymers*, **68**, 121–129.
- Li, B. et al. (2001a) *J. Am. Chem. Soc.* **123**, 11991–11998.
- Li, B. et al. (2001b) *J. Mol. Biol.* **305**, 581–592.
- Lovell, S.C. et al. (2003) *Proteins: Struct. Func. Genet.*, **50**, 437–450.
- Luan, C.-H. et al. (1990) *Biopolymers*, **29**, 1699–1706.
- Luan, C.-H. et al. (1992) *Biopolymers*, **32**, 1251–1261.
- Matthew, J.B. et al. (1985) *CRC Crit. Rev. Biochem.*, **18**, 91–197.
- Meyer, D.E. and Chilkoti, A. (1999) *Nat. Biotechnol.*, **17**, 1112–1115.
- Meyer, D.E. and Chilkoti, A. (2002) *Biomacromolecules*, **3**, 357–367.
- Meyer, D.E. et al. (2001a) *Cancer Res.*, **61**, 1548–1554.
- Meyer, D.E. et al. (2001b) *Biotechnol. Prog.*, 720–728.
- Nath, N. and Chilkoti, A. (2001) *J. Am. Chem. Soc.*, **123**, 8197–8202.
- Pattanaik, A. et al. (1991) *Biochem. Biophys. Res. Commun.*, **178**, 539–545.
- Pflugrath, J.W. et al. (1986) *J. Mol. Biol.* **189**, 383–386.
- Radzicka, A. and Wolfenden, R. (1988) *Biochemistry*, **27**, 1664–1670.
- Roseman, M.A. (1988) *J. Mol. Biol.*, **200**, 513–522.
- Urry, D.W. (1988) *J. Protein Chem.*, **7**, 1–34.
- Urry, D.W. (1992) *Prog. Biophys. Mol. Biol.*, **57**, 23–57.
- Urry, D.W. (1993) *Angew. Chem. Int. Ed. Engl.*, **32**, 819–841.
- Urry, D.W. (1997) *J. Phys. Chem.*, **101**, 11007–11028.
- Urry, D.W. et al. (1985) *Biopolymers*, **24**, 2345–2356.
- Urry, D.W. et al. (1991) *J. Am. Chem. Soc.*, **113**, 4346–4348.
- Urry, D.W. et al. (1997) *J. Am. Chem. Soc.* **119**, 1161–1162.
- Weisbecker, C.S. et al. (1996) *Langmuir*, **12**, 3763–3772.
- Wiegand, G. et al. (1995) *J. Mol. Biol.*, **247**, 99–110.
- Word, J.M. et al. (1999) *J. Mol. Biol.*, **285**, 1711–1733.

Received June 5, 2003; accepted October 21, 2003

Edited by Valerie Daggett